Submitted: 03 January, 2026 Accepted: 24 March, 2026 Published: 30 July, 2026 DOI:10.22514/jomh.2026.062

ORIGINAL RESEARCH

JOMH Journal of Men's Health

Integrated proteomics identifies a dysfunctional acrosomal module associated with impaired acrosome reaction in asthenozoospermia

Andu Zhu[1,2], Jie Zhu[2,3], Dongdong Jin[2,3,*]

[1]Department of Clinical Laboratory, Suzhou Ninth People's Hospital, 215200 Suzhou, Jiangsu, China
[2]Soochow University, 215123 Suzhou, Jiangsu, China
[3]Department of Obstetrics and Gynecology, Suzhou Ninth People's Hospital, 215200 Suzhou, Jiangsu, China

***Correspondence**
jindongdong1076@suda.edu.cn
(Dongdong Jin)

Abstract

Background: Asthenozoospermia, a primary cause of male infertility, is characterized not only by reduced sperm motility, but also by functional impairments, particularly defects in the acrosome reaction. However, the molecular mechanisms underlying acrosome reaction dysfunction remain incompletely elucidated. This study aimed to identify key dysregulated proteins in asthenozoospermia and to elucidate their association with acrosome reaction defects using an integrated approach of proteomics, bioinformatics, and functional validation. **Methods**: Semen samples were collected from normozoospermic men and patients with asthenozoospermia. Differential expression profiling was performed using quantitative proteomics, following an initial assessment of sperm concentration and motility via a computer-assisted sperm analysis (CASA) system. From the pool of differentially expressed proteins, we identified a core set enriched in acrosome reaction-related pathways. The expression of key candidates from this set was confirmed by Western Blot, and a protein-protein interaction (PPI) network analysis was employed to delineate a core functional module. Finally, the calcium ionophore A23187 was utilized to induce the acrosome reaction *in vitro*, with the spontaneous (sAR) and induced (iAR) acrosome reaction rates evaluated by fluorescein isothiocyanate-labeled peanut agglutinin (FITC-PNA) staining. **Results**: Proteomic analysis revealed a significantly downregulated acrosomal protein module in asthenozoospermia, a finding confirmed by Western Blot. PPI network analysis indicated these proteins form a functional interactome. The asthenozoospermic group showed significantly lower sperm motility and concentration. Critically, these sperm displayed a characteristically impaired acrosomal response, with a lower induced reaction rate (iAR) and a spontaneous rate (sAR) that showed an increasing trend without statistical significance, revealing defects in both acrosomal function and stability. **Conclusions**: This study reveals that the coordinated downregulation of an acrosomal functional module underpins the sAR with an increasing trend without statistical significance, low iAR paradox in asthenozoospermia, thereby providing molecular insights into its pathology and identifying new targets for diagnosis and therapy.

Keywords

Asthenozoospermia; Acrosome reaction; Proteomics; Protein interaction maps; Infertility; Male

1. Introduction

Male infertility poses a significant global health challenge, with male factors contributing to approximately 50% of cases among affected couples [1]. Asthenozoospermia, the most prevalent clinical presentation, is diagnostically defined by reduced sperm motility [2]. However, growing evidence underscores its association with broader functional defects, particularly in the acrosome reaction—a pivotal but frequently overlooked cause of fertilization failure. This crucial calcium-dependent exocytotic event, triggered by sperm-zona pellucida binding, is indispensable for penetrating the oocyte's vestments [3, 4]. A fertile sperm maintains acrosomal integrity until the fertilization site, then executes the reaction precisely. In contrast, dysfunctional sperm may present a functional paradox: "acrosome reaction insufficiency" (failure to initiate when needed) or "premature acrosome reaction" (untimely initiation, abolishing fertilizing potential) [5, 6]. While both lead to failed fertilization, their specific molecular mechanisms in asthenozoospermia remain inadequately defined.

High-throughput proteomics offers a powerful strategy to systematically map molecular alterations in male infertility,

enabling the identification of key proteins and pathways by comparing physiological and pathological sperm proteomes. Although prior studies have identified candidate biomarkers for asthenozoospermia using this technology [7, 8], they largely stop at identification. A critical gap remains in the integrative, module-based analysis of these findings and their correlation with concrete sperm functional impairments, particularly the dysregulation of acrosome reactions (spontaneous versus induced). Notably, while several proteins—including Sperm acrosome membrane-associated protein 1 (SPACA1), Sperm equatorial segment protein 1 (SPESP1), Acrosin (ACR), Acrosin-binding protein (ACRBP), and Ropporin-1B (ROP1B)—have been independently associated with sperm function and acrosome biology [9–12], the hypothesis that they act as a concerted functional module whose dysregulation underlies acrosomal defects in asthenozoospermia remains elusive.

Based on this premise, we hypothesized that a coordinately dysregulated "acrosome functional module" constitutes the core molecular basis linking aberrant sperm motility to acrosome reaction dysfunction in asthenozoospermia. To test this, we employed an integrated strategy combining proteomic profiling, bioinformatic network analysis, Western blot validation, and systematic functional assessments of sperm motility and acrosome status (sAR and iAR). This study was designed to systematically identify dysregulated acrosome-related proteins in asthenozoospermia, to validate and define a core dysfunctional protein module, and to establish its functional link with acrosome reaction defects. Our findings are expected to provide novel molecular insights into the pathogenesis of asthenozoospermia and to identify potential targets for future diagnostic and therapeutic development.

2. Materials and methods

2.1 Source of semen samples

Semen samples were prospectively recruited from men undergoing routine fertility evaluation at Suzhou Ninth People's Hospital (Suzhou, China). The recruitment period for this study spanned from 01 March 2024, to 15 September 2025. All samples were obtained via masturbation into sterile collection containers, following a recommended abstinence period of 2–7 days. After liquefaction at 37 °C for 30 minutes, the fresh samples were subjected to routine semen analysis.

2.2 Participant grouping and selection criteria

Participants were classified into two groups based on the fifth edition of the World Health Organization (WHO) Laboratory Manual for the Examination and Processing of Human Semen [13]. Individuals in the normozoospermia group exhibited normal semen parameters, defined by a sperm concentration $\geq 15 \times 10^6$/mL, progressive motility (PR) $\geq$32%, total motility (PR + non-progressive motility, NP) $\geq$40%, and normal morphology $\geq$4%. The asthenozoospermia group included subjects with normal sperm concentration ($\geq 15 \times 10^6$/mL) and morphology ($\geq$4%), but with a significant reduction in either progressive motility (PR $<$32%) and/or total motility (PR + NP $<$40%). Exclusion criteria were applied to maintain cohort homogeneity, encompassing conditions such as varicocele, genital tract infections, chromosomal abnormalities, endocrine disorders, and a recent history of smoking, alcohol abuse, or medication use that could adversely affect sperm function.

2.3 Pro data independent acquisition (DIA)-based quantitative proteomics

A total of 10 normozoospermic controls and 10 asthenozoospermic patients were enrolled as the independent discovery cohort for Pro DIA-based quantitative proteomic profiling, all of whom met the inclusion and exclusion criteria defined in Section 2.2. Baseline clinical characteristics of this cohort were consistent with the validation cohort used for acrosome reaction assays and Western blot analysis. Total protein was extracted from the samples, with an aliquot reserved for concentration measurement and sodium dodecyl sulfate polyacrylamide gel electrophoresis (SDS-PAGE) analysis, and the remainder digested with trypsin at a mass ratio of 1:50 (trypsin:protein) for 12 h at 37 °C. The samples were desalted on SOLA™ SPE. After drying under vacuum, samples were resuspended and indexed retention time (iRT) peptides (1:10) were added.

The proteomic data analysis was performed by Shanghai OE Biotech Co., Ltd. (Shanghai, China). All analyses were performed by a Tims TOF Pro mass spectrometer (Bruker Daltonics, Bremen, HB, Germany) equipped with an Easyspray source (Thermo, USA). Samples were loaded on a C18 column (15 cm $\times$ 75 μm) using an EASY-nLCTM 1200 system (Thermo, San Jose, CA, USA). The flow rate was 300 nL/min and linear gradient was set as follows: 0~20 min, 5–22% B; 20~24 min, 22–37% B; 24~27 min, 37–80% B; 27–30 min, 80% B. Ion mobility was set from 0.7 to 1.3 Vs/cm^2 and the collision energy range from 20 to 59 eV. The (tandem mass spectrometry) MS/MS spectra were recorded from 100 to 1700 m/z.

MS/MS spectra were searched using the Spectronaut Pulsar™ 18.4 (Biognosys, Schlieren, ZH, Switzerland) against the Uniprot Mus Musculus database. Search database-specific parameters were set as follows: Fixed modifications: Carbamidomethyl (C); Variable modification: Oxidation (M) and Acetyl (Protein N-term); Digestion: trypsin; Precursor Qvalue cutoff: 0.01; Protein Qvalue cutoff: 0.01; Missed cleavage: 2; Quantity MS-Level: MS2.

Bioinformatic analysis commenced with quality assessment and preprocessing of the identified proteins, followed by expression and functional analyses. The differentially expressed proteins were functionally annotated using public databases and subjected to Gene Ontology (GO) enrichment, pathway, and protein-protein interaction (PPI) analyses. Gene Ontology (GO) enrichment analysis was performed using the whole genome of human semen proteins as the background gene set, which ensured the comprehensiveness of functional annotation and the reliability of enrichment results for differentially expressed acrosomal-related proteins. Differential expression was visualized by volcano plots, hierarchical clustering heatmaps, and Venn diagrams. Based on these findings, key proteins and pathways were selected for further investiga-

tion and validation.

The mass spectrometry proteomics data generated in this study have been deposited to the ProteomeXchange Consortium via the PRoteomics IDEntifications (PRIDE) [14, 15] partner repository with the dataset identifier PXD075674.

2.4 Protein-protein interaction network

A protein-protein interaction (PPI) network for the target proteins (SPACA1, SPESP1, ACR, ACRBP, ROP1B) was constructed using the online Search Tool for the Retrieval of Interacting Genes/Proteins (STRING) database [16], with the species set to "Homo sapiens" and a minimum interaction confidence score of 0.70. Subsequently, the network data were imported into Cytoscape software for visualization. The CytoHubba plugin was then utilized to identify hub nodes within the network, thereby assessing the functional importance of the target proteins.

2.5 Western blot (WB)

Western blot validation was performed on the same cohort of 10 normozoospermic controls and 10 asthenozoospermic patients used for acrosome reaction functional assays (Section 2.6), with all subjects meeting the identical inclusion and exclusion criteria. For WB analysis, 3 biological replicates per group were randomly selected from this 10:10 cohort for experimental validation and subsequent statistical analysis, and these samples yielded valid and quantifiable WB results. Following liquefaction of the fresh semen samples at 37 °C for 30 min, sperm proteins were extracted using a Sperm Protein Extraction Kit (catalog #EX1620, Solarbio, Beijing, China). A specified amount of protein was separated on 10% SDS-PAGE gels and transferred onto polyvinylidene difluoride (PVDF) membranes. After blocking with 5% non-fat milk for 2 hours at room temperature, the membranes were incubated with specific primary antibodies overnight at 4 °C. The primary antibodies, all rabbit polyclonal, were used at a dilution of 1:2000 and included: anti-ROP1B (Immunoway, catalog #YN4094, Suzhou, Jiangsu, China), anti-ACR (Immunoway, catalog #YC0001, Suzhou, Jiangsu, China; raised against recombinant human ACR protein), anti-ACRBP (Immunoway, catalog #YT3484, Suzhou, Jiangsu, China), anti-SPACA1 (Proteintech, catalog #12829-1-AP, Wuhan, Hubei, China; raised against a human SPACA1 peptide), and anti-SPESP1 (Proteintech, catalog #28010-1-AP, Wuhan, Hubei, China; raised against a human SPESP1 peptide). These commercial antibodies have been validated by their suppliers for Western blot analysis of human samples, and in our study, each produced a single band at the expected molecular weight, confirming specificity. Subsequently, the membranes were incubated for 2 hours at room temperature with a horseradish peroxidase (HRP)-conjugated goat anti-rabbit IgG (H + L) secondary antibody (Beyotime, catalog #A0208) at a dilution of 1:4000. Protein bands were finally visualized using an enhanced chemiluminescence (ECL) kit (catalog #E422-01, Novozan, Nanjing, Jiangsu, China) and quantified using ImageJ software (National Institutes of Health, USA). All Western Blot experiments were independently repeated at least 3 times with biological replicates to ensure the reliability of experimental results.

2.6 Acrosome reaction

Following liquefaction of fresh semen samples at 37 °C for 30 min, sperm were purified using Percoll density gradient centrifugation and washed with pre-warmed Earle's solution [17]. A drop of the washed sperm was smeared onto a slide to serve as the non-capacitated group. The remaining sperm were resuspended in 1.5 mL of Biggers-Whitten-Whittingham (BWW) capacitation medium and incubated in a CO_2 incubator (5% CO_2, 95% air, 37 °C) for 3 h. The capacitated sperm were then divided equally into three 500 μL aliquots. One aliquot was washed with pre-warmed Earle's solution and smeared onto a slide as the capacitated group. The other two aliquots were treated with either A23187 dissolved in dimethyl sulfoxide (DMSO) to a final concentration of 10 μM [18] or an equal volume of DMSO as a control. Both were incubated in the CO_2 incubator for an additional 20 min. Following incubation, the samples were washed with Earle's solution and smeared onto slides to serve as the induced and control groups, respectively. After smearing, the sperm slides were fixed with 4% paraformaldehyde for 10 min and then washed three times with distilled water. Once dry, 600 μL of FITC-PNA was added to each slide, and the slides were incubated for 1 h at 37 °C in the dark [19]. After staining, the slides were washed three times with distilled water. Upon drying, a drop of 4′,6-diamidino-2-phenylindole (DAPI) mounting medium was applied, and a coverslip was placed on top. The results were observed under a fluorescence microscope with an excitation wavelength of 450–490 nm. All assessments of acrosome reaction were performed via blinded counting: the researchers responsible for sperm observation and counting were unaware of the sample grouping information to avoid subjective judgment bias. For each slide, 200 sperm were counted. Sperm that had not undergone the acrosome reaction were characterized by fluorescence over the head's acrosomal region, whereas acrosome-reacted sperm were identified by fluorescence only at the equatorial segment or by a complete absence of fluorescence over the acrosomal region.

2.7 Statistical analyses

The statistical analysis for this study was performed using GraphPad Prism 8.0.2 (GraphPad Software, San Diego, CA, USA). Data are presented as Mean $\pm$ standard deviation (SD). All experimental data were first subjected to the Shapiro-Wilk test for normality verification prior to subsequent statistical analysis. Statistical comparisons between two groups were conducted using an unpaired *t*-test (or Welch's *t*-test if variances were unequal). For multiple-group comparisons, one-way analysis of variance (ANOVA) followed by Tukey's *post-hoc* test was employed. A *p*-value of < 0.05 was considered statistically significant. All experiments were performed with a minimum of three biological replicates per group. For functional enrichment analysis, the hypergeometric distribution test was used to calculate the raw *p*-value for the significant enrichment of functional sets in foreground proteins, and the Benjamini & Hochberg method was further adopted for multiple test correction to obtain the false discovery rate (FDR) as

the adjusted p-value.

3. Results

3.1 Basic semen parameters and acrosomal function characteristics of sperm from patients with asthenozoospermia

3.1.1 Basic semen parameters

Routine semen analysis confirmed the distinct phenotypic profiles of the two cohorts (Table 1, Fig. 1A,B). Both groups met WHO fifth edition standards for sperm concentration and normal morphology, ensuring cohort comparability and excluding confounding effects from oligozoospermia or teratozoospermia. As anticipated, the asthenozoospermic group exhibited profoundly and statistically significant impairments in both progressive and total motility (both $p < 0.0001$), which unequivocally confirmed the clinical diagnosis. The observed difference in sperm concentration, while statistically significant, was not clinically relevant as both groups remained well above the WHO reference limit, a finding consistent with the known heterogeneity of the condition [20].

3.1.2 Assessment of acrosome reaction function

Assessment of acrosomal function revealed a defining functional defect in asthenozoospermic sperm (Table 1, Fig. 1C,D). Although the spontaneous acrosome reaction (sAR) rate was numerically elevated in the asthenozoospermic group, this trend did not reach statistical significance, suggesting a potential instability of the acrosomal membrane and a propensity for premature reaction prior to receiving the correct physiological signals. In stark contrast, upon induction with calcium ionophore A23187, the asthenozoospermic group exhibited a significantly blunted acrosome reaction capacity ($p < 0.01$). This "sAR with an increasing trend but no statistical significance, low iAR" phenotype delineates a dual acrosomal defect in asthenozoospermia, characterized by a propensity for premature acrosomal loss coupled with an inability to mount a robust physiological acrosome reaction.

3.2 Proteomic analysis identifies differentially expressed acrosome-related proteins in asthenozoospermia

To investigate the molecular etiology of asthenozoospermia, particularly the underlying causes of acrosomal function defects, we analyzed semen samples from both groups using Pro DIA-based quantitative proteomics, the complete raw proteomics dataset is available in the PRIDE repository (PXD075674). A total of over 3700 proteins were identified. Using the criteria of a p-value < 0.05 and a fold change ≥ 2.0 or ≤ 0.5, we identified a total of 261 differentially expressed proteins (DEPs), of which 100 were upregulated and 161 were downregulated in the asthenozoospermia group (Fig. 2A, complete dataset available in **Supplementary material 1**). The volcano plot provides a visual overview of the overall distribution of these DEPs, while the hierarchical clustering heatmap illustrates their co-expression patterns and the grouping structure across the samples (Fig. 2B,C).

Gene Ontology (GO) biological process enrichment analysis of these differentially expressed proteins revealed that they were significantly enriched in a series of items closely related to sperm function, including "acrosome reaction" ($p = 6.14 \times 10^{-5}$), "acrosome assembly" ($p = 2.44 \times 10^{-5}$), and "fusion of sperm to egg plasma membrane involved in single fertilization event" ($p = 2.44 \times 10^{-5}$) (Fig. 2D–F). This result suggests that dysregulation of acrosome-related pathways is one of the core molecular events in asthenozoospermia.

A deeper analysis of the downregulated proteome revealed a striking pattern of co-downregulation among several acrosomal proteins with pivotal structural and functional roles, including SPACA1, SPESP1, ACR, ACRBP, and ROP1B (Table 2). Given their concerted and statistically significant decrease in expression, we defined this group as a "dysfunctional acrosomal module" underlying asthenozoospermia. Notably, the coordinated downregulation of this acrosomal module was statistically associated with the acrosomal function defects in asthenozoospermic sperm, and further experimental perturbation studies are required to verify the causal relationship between the dysregulation of these proteins and the impaired acrosome reaction.

TABLE 1. Comparison of semen parameters among study subjects.

Parameter	Normal Control Group	Asthenozoospermic Group
Sperm Concentration (10^6/mL)	132.92 ± 56.73	64.25 ± 31.14**
Total Motility (PR + NP) (%)	72.51 ± 15.67	34.17 ± 7.04****
PR (Progressive Motility) (%)	64.08 ± 15.14	31.25 ± 6.08****
NP (Non-progressive Motility) (%)	5.18 ± 5.82	3.28 ± 1.39
IM (Immotility) (%)	27.49 ± 15.67	67.53 ± 7.04****
Spontaneous Acrosome Reaction Rate (%)	14.45 ± 3.59	15.85 ± 3.75
Induced Acrosome Reaction Rate (%)	37.85 ± 5.12	28.15 ± 3.87**

*Values are presented as mean ± standard deviation. Ten Participants were selected for analysis from each group. Versus control group (**$p < 0.01$, ****$p < 0.0001$). PR: Progressive Motility; NP: Non-progressive Motility.*

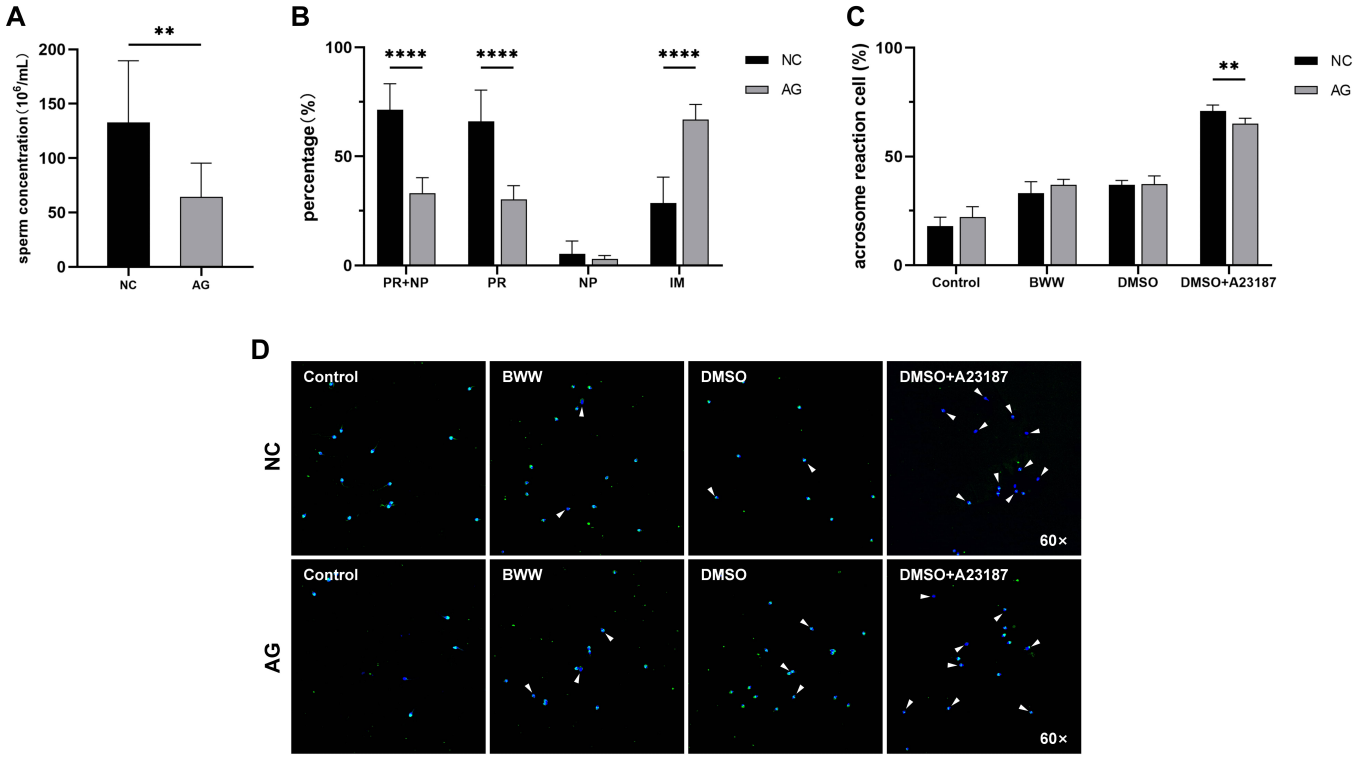

FIGURE 1. Basic parameters and acrosomal function characteristics of sperm from asthenozoospermia patients. NC: Negative Control; AG: Asthenozoospermic Group; Versus control group (**$p < 0.01$, ****$p < 0.0001$). (A) Comparison of sperm concentration between the NC and AG groups. (B) Comparison of basic semen parameters, including total motility (PR + NP), progressive motility (PR), non-progressive motility (NP), and immotility (IM), between the NC and AG groups. (C) Statistical bar chart of spontaneous and induced acrosome reaction counts in the NC and AG groups. (D) Schematic fluorescence confocal microscopy images illustrating spontaneous and induced acrosome reactions. Sperm that had not undergone the acrosome reaction were characterized by fluorescence over the head's acrosomal region, whereas acrosome-reacted sperm were identified by fluorescence only at the equatorial segment or by a complete absence of fluorescence over the acrosomal region, as indicated by the arrows. BWW: Biggers-Whitten-Whittingham capacitation medium; DMSO: dimethyl sulfoxide.

3.3 Protein-protein interaction network analysis and validation of the core acrosomal module

3.3.1 Protein-protein interaction network analysis

From the 261 identified differentially expressed proteins (DEPs) in asthenozoospermic sperm, we implemented a multi-criteria stringent screening strategy to prioritize core acrosome-related proteins for subsequent PPI network analysis, ensuring the biological relevance and statistical robustness of the selected subset. The screening criteria were defined as follows: (1) functional enrichment in acrosome-related pathways: extraction of DEPs annotated to acrosome reaction, acrosome assembly, and acrosomal membrane formation via GO biological process and cellular component enrichment analysis; (2) literature validation of acrosomal function: cross-referencing with published studies to retain only DEPs with well-characterized roles in mammalian sperm acrosome structure and acrosome reaction regulation; (3) statistical significance of downregulation: further filtering for proteins with a significantly decreased expression in asthenozoospermia ($p < 0.01$). Through this tiered selection process, five core downregulated proteins (SPACA1, SPESP1, ACR, ACRBP, ROP1B) were identified as the focus of PPI network analysis, representing a functionally coherent and statistically dysregulated acrosomal protein set. To explore the functional relationships among the five candidate proteins, we constructed a PPI network using the STRING database. The analysis revealed that these proteins form a highly interconnected cluster through known biochemical interactions, rather than acting in isolation (Fig. 3A). Although ROP1B appears as a peripheral node in the direct interaction view, topological analysis confirmed its integration within the module (Fig. 3B–D). Notably, this entire module was identified as a core hub in the global differential protein network, underscoring its central biological importance. It should be noted that the present PPI network analysis is primarily exploratory in nature, intended to delineate potential functional associations among the core acrosomal proteins and generate hypotheses regarding their coordinated roles in acrosome biology, rather than to establish definitive causal molecular interactions.

3.3.2 Validation of key proteins by western blot

To validate the proteomic findings from the independent discovery cohort (10:10), WB analysis was performed on the

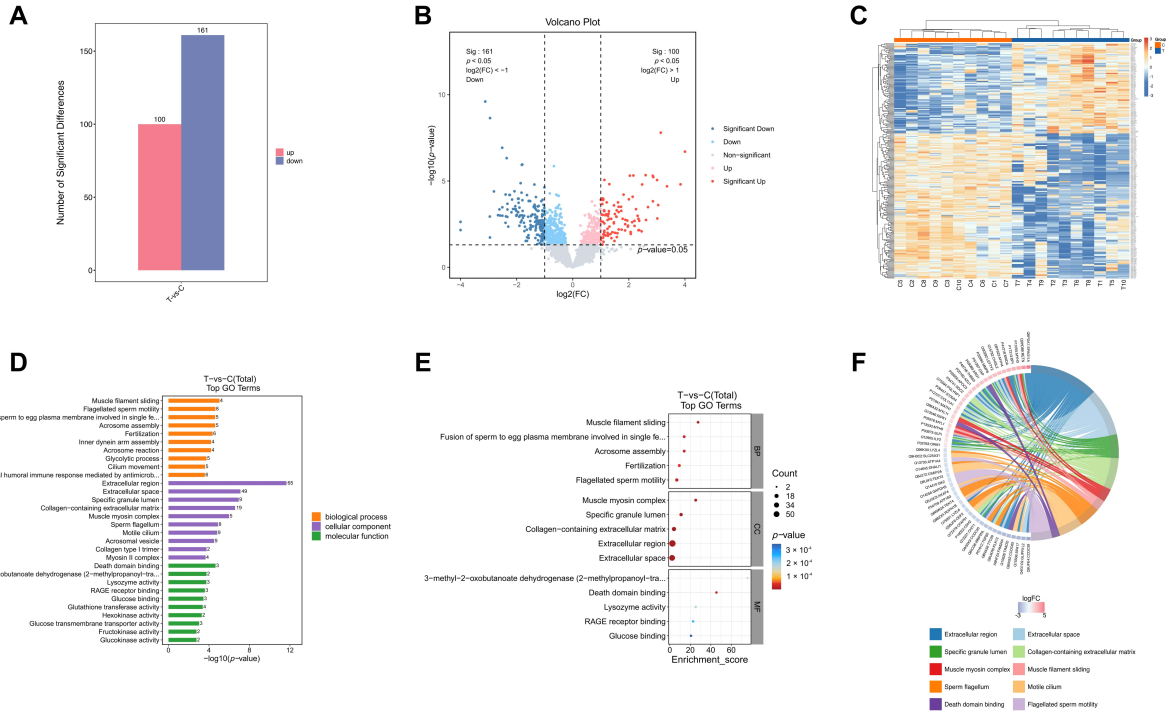

FIGURE 2. Comparative proteomic profiling reveals dysregulated acrosome-associated pathways in asthenozoospermia. (A) Summary of differentially expressed proteins (DEPs) between the asthenozoospermic and control groups. (B) Volcano plot displaying the significance and magnitude of protein expression changes. Significantly upregulated (red) and downregulated (blue) DEPs are highlighted ($p < 0.05$, fold change $\geq$2.0 or $\leq$0.5). (C) Hierarchical clustering of DEPs across samples, demonstrating distinct proteomic signatures between the two groups. (D–F) Gene Ontology (GO) enrichment analysis of DEPs. (D) Bar chart and (E) bubble plot of significantly enriched GO terms, highlighting the strong association of DEPs with acrosome-related biological processes and cellular components. (F) Chord diagram illustrating the specific associations between key DEPs (left) and the most relevant acrosome-related GO terms (right). FC: fold change; RAGE: receptor for advanced glycation endproducts; BP: biological process; CC: cellular component; MF: molecular function.

TABLE 2. Proteomic quantification results of core acrosomal module proteins.

Symbol	Protein Name	Fold Change	*p*-value	*q*-value	GO term
SPACA1	Sperm acrosome membrane-associated protein 1	0.394472600	0.000884219	0.025134104	Acrosome assembly, acrosomal membrane, inner acrosomal membrane
ACR	Acrosin	0.419570456	0.002250947	0.03925565	Acrosome matrix dispersal, acrosome reaction, binding of sperm to zona pellucida, penetration of zona pellucida, single fertilization, acrosomal matrix
ACRBP	Acrosin-binding protein	0.440612705	0.001982919	0.036352174	Acrosome assembly, fertilization, acrosomal membrane, acrosomal vesicle
ROP1B	Ropporin-1B	0.450480012	0.002486337	0.040069977	Acrosome reaction, flagellated sperm motility, sperm capacitation
SPESP1	Sperm equatorial segment protein 1	0.479604134	0.002703141	0.041324245	Acrosome reaction, fertilization, fusion of sperm to egg plasma membrane involved in single fertilization, sperm-egg recognition, acrosomal vesicle

Fold change represents the ratio of protein expression levels in the asthenozoospermic group compared with the normal control group. p-value indicates the statistical significance of the difference in protein expression between the asthenozoospermic group and the control group. GO term indicates the significantly enriched Gene Ontology terms for the protein, encompassing its involved biological process, associated cellular component, and potential molecular function. GO: Gene Ontology.

same 10:10 cohort used for acrosome reaction assays, with 3 biological replicates per group randomly selected for experimental validation and statistical analysis. The results were entirely consistent with the omics data (Fig. 3E,F). Uncropped blots are available in **Supplementary material 2**. In addition, the full membranes and sample information corresponding to each lane can be found in **Supplementary material 3**. Quantitative analysis of the grayscale values of the protein bands clearly demonstrated that the expression levels of SPACA1, SPESP1, ACR, ACRBP, and ROP1B were all significantly lower in the asthenozoospermia group compared with the normal control group ($p < 0.0001$). This thus confirmed, at the protein level, the coordinated dysregulation of this acrosomal module in asthenozoospermia. These results further confirmed the significant statistical correlation between the downregulated expression of the SPACA1-SPESP1-ACR-ACRBP-ROP1B module and the defective acrosome reaction in asthenozoospermia, while the causal regulatory mechanisms underlying this association remain to be elucidated in subsequent functional studies.

4. Discussion

By integrating high-throughput proteomics, bioinformatics, and functional validation, this study systematically deciphered the molecular basis of acrosomal dysfunction in asthenozoospermia. We confirmed the characteristic motility deficiency and, more critically, identified a dual acrosomal defect through simultaneous sAR and iAR assessment. The sAR showed an increasing trend without statistical significance in asthenozoospermic sperm, which implies a potential acrosomal instability that may lead to premature enzyme release during sperm transit and consequent loss of fertilizing capacity [21]. In contrast, diminished iAR reflects an inability to mount a competent acrosome reaction upon physiological stimulation, a condition termed "acrosome reaction insufficiency" [22, 23]. These seemingly paradoxical defects jointly contribute to fertilization failure in asthenozoospermia. Our findings underscore that fertility assessment must extend beyond motility to include a comprehensive evaluation of acrosomal function, particularly the sAR/iAR ratio, which holds significant clinical relevance.

The central finding of this study is the identification of a coordinately downregulated "acrosome functional module" in asthenozoospermia. Unlike previous approaches focused on individual proteins, our modular analysis strategy aligns more closely with the biological reality that proteins operate within interconnected networks to perform complex functions. Acrosin (ACR), the core catalytic component of this module, is the key enzyme responsible for hydrolyzing the zona pellucida. The activation and precise localization of its precursor, proacrosin, are indispensable for a successful acrosome reaction [24]. The significant downregulation of ACR observed in our study, therefore, directly undermines the sperm's penetrating ability. Acrosin-binding protein (ACRBP), which anchors proacrosin within the acrosomal matrix, is indispensable for

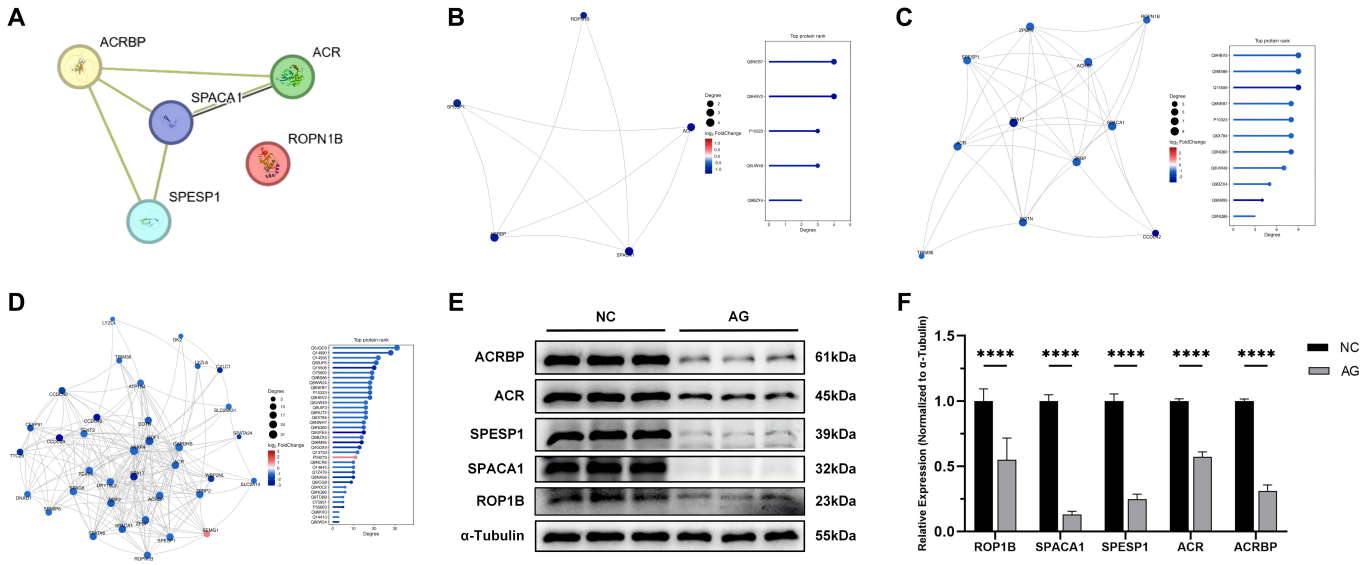

FIGURE 3. Protein-protein interaction network analysis and validation of a core acrosomal module in asthenozoospermia. (A) PPI network of the candidate proteins from the STRING database. Despite the absence of a direct binary link to ROP1B (UniProt nomenclature, corresponding to ROPN1B in STRING), its co-downregulation and functional coherence warrant its inclusion in the functional module. (B–D) Topological analysis demonstrating the hub status of the core module within PPI networks of increasing scope: (B) the five candidates, (C) all acrosome reaction-related proteins, and (D) all sperm-related proteins. The module's centrality is maintained, highlighting its fundamental role. (E) Representative Western Blot images of the five core module proteins in normal (NC) and asthenozoospermic (AG) sperm. (F) Quantitative analysis of Western Blot data (mean ± SD; unpaired *t*-test, ****$p < 0.0001$), confirming the coordinated downregulation of the entire module in asthenozoospermia, consistent with proteomic findings. SPACA1: Sperm acrosome membrane-associated protein 1; SPESP1: Sperm equatorial segment protein 1; ACR: Acrosin; ACRBP: Acrosin-binding protein; ROP1B: Ropporin-1B; AG: Asthenozoospermia Group; NC: Negative Control.

maintaining its stability and regional distribution [25]. The observed downregulation of ACRBP likely causes mislocalization and aberrant activation of proacrosin. This dysregulation may represent a shared molecular defect underlying the dual acrosomal phenotypes of sAR with an increasing trend, but no statistical significance, and diminished iAR. Sperm acrosome membrane-associated protein 1 (SPACA1) and Sperm equatorial segment protein 1 (SPESP1) are key functional proteins on the acrosomal membrane. SPACA1 facilitates acrosomal membrane remodeling during the acrosome reaction [26], while SPESP1, which resides in the equatorial segment, is essential for sperm-oocyte membrane fusion [27]. The downregulation of these two proteins may impair the efficiency of acrosomal exocytosis and the success rate of sperm-oocyte fusion, respectively. Ropporin-1B (ROP1B), a fibrous sheath protein, is thought to play a role in maintaining the structural integrity of the acrosome [28, 29]. Its reduced expression may lead to a fragile acrosomal structure that is prone to premature rupture, providing a structural explanation for the elevated sAR. More importantly, Protein-Protein Interaction (PPI) network analysis confirmed that these five proteins form a tightly interconnected functional unit. This suggests that their coordinated downregulation is not coincidental, but may stem from a common upstream regulatory abnormality (such as dysregulated transcription or aberrant post-translational modification), ultimately leading to a systemic collapse in both the structural stability and functional execution of the acrosome.

Our findings hold potential clinical value. The SPACA1-SPESP1-ACR-ACRBP-ROP1B module represents a promising novel molecular signature for assessing acrosomal function in patients with asthenozoospermia. In the future, by measuring the expression levels of these proteins, it may be possible to more accurately predict a patient's acrosome reaction potential, thereby providing a basis for individualized treatment strategies in assisted reproductive technologies, such as determining the necessity for Intracytoplasmic Sperm Injection (ICSI).

Of course, this study has several limitations. First, the samples were sourced from a single medical center, and thus our findings require validation in a broader population. Second, the acrosome reaction in this study was induced using the calcium ionophore A23187, an artificial non-physiological stimulant that mediates non-specific calcium influx into sperm to trigger acrosomal exocytosis, bypassing the natural receptor-mediated signaling cascades activated by physiological inducers such as progesterone and zona pellucida glycoproteins. This induction method reflects the sperm's overall capacity for calcium-dependent acrosomal exocytosis, rather than its specific response to physiological ovarian/oviductal signals, and cannot fully recapitulate the spatiotemporal control and signal specificity of the acrosome reaction in the female reproductive tract. Third, while we identified a correlation between the dysregulation of the protein module and functional defects, the specific upstream regulatory mechanisms, such as those involving transcription factors or non-coding RNAs, remain unclear. Fourth, the precise molecular interactions among the proteins within this module during the acrosome reaction, and how their dysregulation specifically leads to an elevated sAR and a reduced iAR, warrant further elucidation through functional gain- and loss-of-function experiments, such as gene knockout and *in vitro* rescue assays. Additionally, future studies will supplement functional assessments using progesterone and recombinant zona pellucida glycoproteins as physiological inducers to validate the acrosomal dysfunction of asthenozoospermic sperm under more physiologically relevant conditions.

5. Conclusions

In summary, this study is the first to systematically reveal the coordinated downregulation of an "acrosome functional module", composed of SPACA1, SPESP1, ACR, ACRBP, and ROP1B, in asthenozoospermia. The dysregulation of this module is a pivotal molecular event leading to decreased acrosomal stability and impaired acrosome reaction capacity, thereby providing a molecular explanation for the "sAR with an increasing trend but no statistical significance, and the low iAR" functional paradox observed in the sperm of asthenozoospermic patients. Our research not only deepens the understanding of the pathogenic mechanisms of asthenozoospermia, but also establishes a solid theoretical foundation for the development of novel diagnostic biomarkers and therapeutic targets.

AVAILABILITY OF DATA AND MATERIALS

The mass spectrometry proteomics data generated in this study have been deposited in the ProteomeXchange Consortium via the PRIDE partner repository under the dataset identifier PXD075674. All other data generated or analyzed during this study are included in this published article and its supplementary information files.

AUTHOR CONTRIBUTIONS

DDJ and ADZ—designed the research study. ADZ—performed the research; analyzed the data. JZ—provided help and advice on the experimental design and data interpretation. ADZ and JZ—wrote the manuscript. All authors contributed to editorial changes in the manuscript. All authors read and approved the final manuscript.

ETHICS APPROVAL AND CONSENT TO PARTICIPATE

The present study protocol was reviewed and approved by The Clinical Medical Research Ethics Committee of the Ninth People's Hospital of Suzhou (Approval No. KY2023-025-01). Prior to inclusion, all participants provided written informed consent. This study was conducted in strict accordance with the principles of the Declaration of Helsinki for medical research involving human subjects.

ACKNOWLEDGMENT

We are grateful to the Department of Clinical Laboratory, The Ninth People's Hospital of Suzhou, for supplying the human semen samples.

FUNDING

This research was funded by the National Key Laboratories Project of China (Grant No. GZK12024031) and supported by the Scientific Research Project of Suzhou Ninth People's Hospital (Grant No. YK202322).

CONFLICT OF INTEREST

The authors declare no conflict of interest.

SUPPLEMENTARY MATERIAL

Supplementary material associated with this article can be found, in the online version, at https://oss.jomh.org/files/article/2082735051642945536/attachment/Supplementary%20material.zip.

REFERENCES

[1] Ferlin A, Calogero AE, Krausz C, Lombardo F, Paoli D, Rago R, *et al*. Management of male factor infertility: position statement from the Italian Society of Andrology and Sexual Medicine (SIAMS): endorsing organization: Italian Society of Embryology, Reproduction, and Research (SIERR). Journal of Endocrinological Investigation. 2022; 45: 1085–1113.

[2] Cavarocchi E, Whitfield M, Chargui A, Stouvenel L, Lores P, Coutton C, *et al.* The sodium/proton exchanger SLC9C1 (sNHE) is essential for human sperm motility and fertility. Clinical Genetics. 2021; 99: 684–693.

[3] Mo L, Wu H, Zhang M, Zhang P, Peng W, He Y, *et al*. The mechanism of oxidative stress in asthenozoospermia and antioxidant strategies: a review. Frontiers in Endocrinology. 2025; 16: 1670762.

[4] Cavarocchi E, Drouault M, Ribeiro JC, Simon V, Whitfield M, Toure A. Human asthenozoospermia: update on genetic causes, patient management, and clinical strategies. Andrology. 2025; 13: 1044–1064.

[5] Esteves SC. Relationship of *in vitro* acrosome reaction to sperm function: an update. The Open Reproductive Science Journal. 2011; 3: 72–84.

[6] Azizi Z, Soleimani Mehranjani M, Shariatzadeh MA, Najdi N, Azimi AS. Papaverine enhances sperm quality in asthenospermia by reducing oxidative stress and inflammation while regulating the expression of apoptosis-related genes during cryopreservation. Cryobiology. 2025; 121: 105329.

[7] Yang J, Liu Q, Yu B, Han B, Yang B. 4D-quantitative proteomics signature of asthenozoospermia and identification of extracellular matrix protein 1 as a novel biomarker for sperm motility. Molecular Omics. 2022; 18: 83–91.

[8] Martinez-Heredia J, de Mateo S, Vidal-Taboada JM, Ballesca JL, Oliva R. Identification of proteomic differences in asthenozoospermic sperm samples. Human Reproduction. 2008; 23: 783–791.

[9] Agil M, Pardede BP, Purwantara B, Arifiantini RI, Hasbi H, Sonjaya H, *et al.* Sperm acrosome-associated 1 (SPACA1) mRNA and protein molecules deficiency indicate low fertility and semen quality of Bali bulls (sondaicus). Theriogenology. 2025; 233: 80–87.

[10] He J, Lin X, Tan C, Li Y, Su L, Lin G, *et al*. Molecular insights into sperm head shaping and its role in human male fertility. Human Reproduction Update. 2025; 31: 307–332.

[11] Hua R, Xue R, Liu Y, Li Y, Sha X, Li K, *et al.* ACROSIN deficiency causes total fertilization failure in humans by preventing the sperm from penetrating the zona pellucida. Human Reproduction. 2023; 38: 1213–1223.

[12] Corda PO, Moreira J, Howl J, Oliveira PF, Fardilha M, Silva JV. Differential proteomic analysis of human sperm: a systematic review to identify candidate targets to monitor sperm quality. World Journal of Men's Health. 2024; 42: 71–91.

[13] World Health Organization. WHO laboratory manual for the examination and processing of human semen. 5th edn. World Health Organization: Geneva. 2010.

[14] Perez-Riverol Y, Bandla C, Kundu DJ, Kamatchinathan S, Bai J, Hewapathirana S, *et al*. The PRIDE database at 20 years: 2025 update. Nucleic Acids Research. 2025; 53: D543–D553.

[15] Deutsch EW, Bandeira N, Perez-Riverol Y, Sharma V, Carver JJ, Mendoza L, *et al*. The ProteomeXchange consortium in 2026: making proteomics data FAIR. Nucleic Acids Research. 2026; 54: D459–D469.

[16] Zou C, Xu S, Geng H, Li E, Sun W, Yu D. Bioinformatics analysis identifies potential hub genes and crucial pathways in the pathogenesis of asthenozoospermia. BMC Medical Genomics. 2022; 15: 252.

[17] Le Lannou D, Blanchard Y. Nuclear maturity and morphology of human spermatozoa selected by Percoll density gradient centrifugation or swim-up procedure. Journal of Reproduction and Fertility. 1988; 84: 551–556.

[18] Kawai Y, Takeiri A, Suzuki T, Suzuki Y, Miyake M. Anti-mouse sperm monoclonal antibody, A-1, inhibits sperm capacitation, acrosome reaction and calcium influx into spermatocytes. Biological and Pharmaceutical Bulletin. 2000; 23: 922–925.

[19] Zhu Z, Li R, Wang L, Zheng Y, Hoque SAM, Lv Y, *et al*. Glycogen synthase kinase-3 regulates sperm motility and acrosome reaction via affecting energy metabolism in goats. Frontiers in Physiology. 2019; 10: 968.

[20] Zhou D, Wu H, Wang L, Wang X, Tang S, Zhou Y, *et al*. Deficiency of MFSD6L, an acrosome membrane protein, causes oligoasthenoteratozoospermia in humans and mice. Journal of Genetics and Genomics. 2024; 51: 1007–1019.

[21] Guerra-Carvalho B, Carrageta DF, Mauricio T, Pereira SC, Barros A, Carvalho RA, *et al*. Metabolomics analysis of human spermatozoa reveals impaired metabolic pathways in asthenozoospermia. European Journal of Clinical Investigation. 2024; 54: e14289.

[22] Zeginiadou T, Papadimas J, Mantalenakis S. Acrosome reaction: methods for detection and clinical significance. Andrologia. 2000; 32: 335–343.

[23] Khan MR, Shah AA, Al Smadi MA, Ludwig N, Fischer U, Abdul-Khaliq H, *et al*. Identifying potential genetic biomarkers for sperm dysfunction through whole-genome sequencing. Scientific Reports. 2025; 15: 36476.

[24] Quan R, Wu X, Zhang J, Liu R, Han J, Liu D. Extraction, purification, biological effects and applications of acrosin: a review. Frontiers in Cellular and Infection Microbiology. 2025; 15: 1596356.

[25] Zhang M, Chiozzi RZ, Bromfield EG, Heck AJ, Helms JB, Gadella BM. Characterization of acrosin and acrosin binding protein as novel CRISP2 interacting proteins in boar spermatozoa. Andrology. 2023; 11: 1460–1471.

[26] Chen P, Saiyin H, Shi R, Liu B, Han X, Gao Y, *et al*. Loss of SPACA1 function causes autosomal recessive globozoospermia by damaging the acrosome-acroplaxome complex. Human Reproduction. 2021; 36: 2587–2596.

[27] Iniesta-Cuerda M, Nevoral J, Krapf D, Garde J, Soler-Valls AJ, Yeste M. Decoding a novel non-enzymatic protein acetylation mechanism in sperm that is essential for fertilizing potential. Biological Research. 2025; 58: 30.

[28] Li Y, Lu Z, Li J, Cheng L, Ye Y, Xu S, *et al.* Sperm metabolomic signatures of asthenozoospermia and teratozoospermia in Chinese reproductive-age men. Scientific Reports. 2025; 15: 23932.

[29] Nedelcu S, Vitthala S, Maheshwari A. Lab-based semen parameters as predictors of long-term health in men—a systematic review. Human Reproduction Open. 2024; 2024: hoae066.

How to cite this article: Andu Zhu, Jie Zhu, Dongdong Jin. Integrated proteomics identifies a dysfunctional acrosomal module associated with impaired acrosome reaction in asthenozoospermia. Journal of Men's Health. 2026; 22(7): 83-91. doi: 10.22514/jomh.2026.062.